Revisiting plane Couette-Poiseuille flows of a piezo-viscous fluid

Sergey A. Suslov [a,*] and Thien Duc Tran [b]

[a] *Department of Mathematics and Computing and Computational Engineering and Science Research Centre, University of Southern Queensland, Toowoomba, Queensland 4350, Australia*

[b] *Computational Engineering and Science Research Centre, University of Southern Queensland, Toowoomba, Queensland 4350, Australia*

Abstract

We re-examine fully developed isothermal unidirectional plane Couette-Poiseuille flows of an incompressible fluid whose viscosity depends linearly on the pressure as previously considered in [1]. We show that the conclusion made there that, in contrast to Newtonian and power-law fluids, piezo-viscous fluids allow multiple solutions is not justified, and that the inflection velocity profiles reported in [1] cannot exist. Subsequently, we undertake a systematic parametric study of these flows and identify three distinct families of solutions which can exist in the considered geometry. One of these families has no similar counterpart for fluids with pressure-independent viscosity. We also show that the critical wall speed exists beyond which Poiseuille-type flows are impossible regardless of the magnitude of the applied pressure gradient. For smaller wall speeds channel choking occurs for Poiseuille-type flows at large pressure gradients. These features distinguish drastically piezo-viscous fluids from their Newtonian and power-law counterparts.

Key words: pressure-dependent viscosity, piezo-viscous fluid, plane Couette-Poiseuille flow

1 Introduction

Piezo-viscous fluids (i.e. fluids whose viscosity depends strongly on the pressure) form a very interesting rheological class. The possibility of the existence

* Corresponding author
Email address: ssuslov@usq.edu.au (Sergey A. Suslov).

of such fluids in nature has been discussed by various authors for centuries [2–4]. More recently, the fluids exhibiting noticeable dependence of their viscosity on the pressure were found in technological applications such as polymer processing [5] and journal bearing lubrication [6,7]. Besides, geo-fluids such as magma and gases forming Jovial planets which are subject to large pressures are also candidates for this class of fluids. Due to the practical importance of piezo-viscous fluids the number of studies dealing with them increase steadily. Perhaps the most comprehensive cycle of recent works considering flows of such fluids both mathematically from the point of view of existence and well-posedness and numerically are by Hron, Málek, Rajagopal and collaborators [1,8–12]. Earlier studies include [13–15], to name a few. It is argued in these references that even though the fluid can exhibit a strong dependence of viscosity on pressure its compressibility frequently is much weaker. Therefore such fluids can be considered as effectively incompressible, at least for the purpose of studying the piezo-viscous effects [1,16]. Such approach will also be adopted in the present work.

Simple shear flows of piezo-viscous fluids were considered in [1] for two rheological models which assumed the viscosity to be an exponential or linear function of the pressure. It was found in [1] that fully developed solutions can only exist for the linear constitutive law. Later, Renardy [16] confirmed this finding and formulated a general proof that fully-developed plane flows whose velocity is independent of the longitudinal coordinate can exist only for viscosity which depends linearly on the pressure. The major concern regarding this model is that it does not guarantee positive definiteness of the viscosity which requires the pressure to remain positive. Such a constraint is not present for incompressible fluids with pressure-independent rheology for which the pressure is defined up to an arbitrary additive constant. Therefore, special care has to be taken in modelling piezo-viscous fluids to monitor positive-definiteness of the pressure. This will be done in the present work.

It was shown in [1] and [16] that fully developed plane flows of piezo-viscous fluids require exponential dependence of the pressure on the downstream coordinate. While this solution excludes the existence of the negative pressure its physical relevance is still of some concern expressed in [17]: since the pressure and thus viscosity tend to zero exponentially quickly along the channel, the fluid effectively becomes inviscid. This is unlikely to happen in reality. Nevertheless we believe that simple solutions discussed in [1,16] and derived in the present work form an important conceptual and benchmark set for the piezo-viscous rheological model. Therefore here we re-visit and correct previously known results for plane Couette-Poiseuille flows of piezo-viscous fluids, systematically classify all possible solutions and report new remarkable features which distinguish simple piezo-viscous flows from their pressure-independent counterparts. Additionally, we investigate the solutions corresponding to the shear-thinning variant of the rheological model and compare the results with

those obtained for a shear-independent formulation.

2 Problem definition and governing equations

Consider a flow of an incompressible fluid with the pressure-dependent viscosity between two parallel horizontal plates separated by the distance $2L$ from each other. The top plate moves with velocity V^* from left to right, the bottom plate is stationary. The pressure gradient $\nabla\pi$ is applied along the channel which (depending on its direction) can either enhance or partially suppress the fluid flow caused by the motion of the upper wall. The flow is described by the following equations [1]

$$\rho\frac{d\mathbf{u}}{dt} = -\nabla\pi + \nabla\cdot\left(2\mu(\pi)|\mathbf{D}|^{p-2}\mathbf{D}\right)\,, \tag{1}$$

$$\nabla\cdot\mathbf{u} = 0\,, \tag{2}$$

where we neglect the gravity and assume that the velocity field $\mathbf{u}$ is two-dimensional with components (u, v) in the (x, y) directions, respectively. We choose the coordinate system in such a way that the x and y axes have positive right and upward directions, respectively, and the horizontal centre-plane of a channel is located at $y = 0$. In equation (1),

$$\mathbf{D} = \frac{1}{2}\begin{bmatrix} 2\frac{\partial u}{\partial x} & \frac{\partial u}{\partial y}+\frac{\partial v}{\partial x} \\ \frac{\partial u}{\partial y}+\frac{\partial v}{\partial x} & 2\frac{\partial v}{\partial y}\end{bmatrix}\,, \tag{3}$$

$$|\mathbf{D}| = \frac{1}{2}\sqrt{2\left(\frac{\partial u}{\partial x}\right)^2 + 2\left(\frac{\partial v}{\partial y}\right)^2 + \left(\frac{\partial u}{\partial y}+\frac{\partial v}{\partial x}\right)^2}\,. \tag{4}$$

The value of the exponent p defines the shear-dependent properties of a fluid: $p \lessgtr 2$ corresponds to shear-thinning and shear-thickening fluids, respectively. In this paper we will consider in detail two cases: the shear-independent fluid with $p = 2$ and shear-thinning fluid with $p = \frac{3}{2}$.

The governing equations are complemented by the constitutive relations

$$\rho = \text{const.}\,, \quad \mu = a\pi > 0 \tag{5}$$

and the no-slip/no-penetration boundary conditions

$$(u, v) = (0, 0) \text{ at } y = -L \quad \text{and} \quad (u, v) = (V^*, 0) \text{ at } y = L\,. \tag{6}$$

We non-dimensionalise the equations using L, pressure π^* evaluated at $(x,y) = (0,0)$, $u^* = (\pi^*/\rho)^{1/2}$ and $t^* = L(\rho/\pi^*)^{1/2}$, as the scales for length, pressure, velocity and time, respectively, to obtain

$$\frac{\partial \mathbf{u}}{\partial t} + (\mathbf{u}\cdot\nabla)\mathbf{u} = -\nabla\pi + \alpha\nabla\cdot(2\pi|2\mathbf{D}|^{p-2}\mathbf{D})\,, \tag{7}$$

$$\nabla\cdot\mathbf{u} = 0\,, \tag{8}$$

$$(u,v) = (0,0) \text{ at } y = -1 \quad \text{and} \quad (u,v) = (V,0) \text{ at } y = 1\,, \tag{9}$$

$$\pi = 1 \quad \text{at} \quad (x,y) = (0,0)\,, \tag{10}$$

where $V = V^*(\rho/\pi^*)^{1/2}$,

$$\alpha = \frac{a}{2^{p-2}}\left(\frac{\pi^*}{\rho L^2}\right)^{\frac{p-1}{2}} \tag{11}$$

and all symbols now denote the corresponding non-dimensional quantities. Note that α plays the role of the effective inverse Reynolds number. This is easy to see by setting $p = 2$ (which corresponds to the flow of a generalised Newtonian fluid [1]) so that

$$\alpha = a\left(\frac{\pi^*}{\rho L^2}\right)^{\frac{1}{2}} = \frac{a\pi^*}{\rho(\pi^*/\rho)^{1/2}L} = \frac{\mu^*}{\rho u^* L} = \frac{1}{Re}\,. \tag{12}$$

3 Couette-type flows

As was shown in [1] and [16] if the fluid viscosity is a linear function of the pressure, a parallel x-independent steady solution for the velocity field exists away from the channel ends. However the basic flow expressions given in [1] contain a few misprints. Also an incorrect conclusion about the possibility of multiple solutions for the basic flow is made in [1]. To avoid any confusion we re-derive the basic flow expressions here and provide a more structured discussion of the parametric conditions for the existence of various solutions.

Assume that $\mathbf{U} = (U(y), 0)$ and $\pi = \Pi(x,y)$. Then the non-dimensional governing equations become

$$-\frac{\partial\Pi}{\partial x} + \alpha\frac{\partial}{\partial y}\left(\Pi[U']^{p-1}\right) = 0\,, \quad -\frac{\partial\Pi}{\partial y} + \alpha\frac{\partial}{\partial x}\left(\Pi[U']^{p-1}\right) = 0\,, \tag{13}$$

where we assumed that the Couette condition $U'(y) \geq 0$ is satisfied for $-1 \leq y \leq 1$, where prime denotes a derivative with respect to y. The no-slip boundary conditions require that $U(-1) = 0$ and $U(1) = V$. One particular

solution of this system of equations is

$$U(y) = \frac{y+1}{\alpha^{\frac{1}{p-1}}}\,, \quad \Pi = \Pi(\zeta)\,,\ \Pi(0) = 1\,,\ \zeta = x + y\,. \tag{14}$$

This linear velocity profile exists only if the upper plate moves with the non-dimensional velocity $V_c = 2/\alpha^{\frac{1}{p-1}}$. In this case the problem degenerates admitting an arbitrary positively valued function of the argument ζ as a solution for the pressure. In particular, the pressure could be constant (equal to 1 due to the chosen non-dimensionalisation) as is the case in Couette flow of Newtonian fluids. We will discuss the meaning of this ambiguity in section 3.2. If $\alpha^{\frac{1}{p-1}} V \neq 2$ then

$$\frac{\partial \Pi}{\partial x} = \alpha \frac{\partial \Pi}{\partial y}[U']^{p-1} + \alpha(p-1)\Pi[U']^{p-2}U''\,, \quad \frac{\partial \Pi}{\partial y} = \alpha \frac{\partial \Pi}{\partial x}[U']^{p-1}\,. \tag{15}$$

These equations are identical to equations (3.9*ab*) given in [1]. Solving equations (15) for the pressure derivatives we obtain

$$\frac{1}{\Pi}\frac{\partial \Pi}{\partial x} = \frac{\alpha(p-1)[U']^{p-2}U''}{1-\alpha^2[U']^{2(p-1)}}\,, \quad \frac{\partial \Pi}{\partial y} = \frac{\alpha^2(p-1)\Pi[U']^{2p-3}U''}{1-\alpha^2[U']^{2(p-1)}}\,. \tag{16}$$

Further, the first of equations (16) is equivalent to

$$\frac{\partial \ln \Pi}{\partial x} = \frac{1}{2}\frac{d}{dy}\ln\left|\frac{1+\alpha[U']^{p-1}}{1-\alpha[U']^{p-1}}\right| \tag{17}$$

which, upon integration in x, leads to

$$\Pi(x,y) = C_2(y)e^{C_1(y)x}\,, \quad C_1(y) = \frac{1}{2}\frac{d}{dy}\ln\left|\frac{1+\alpha[U']^{p-1}}{1-\alpha[U']^{p-1}}\right|, \quad C_2(y) > 0\,. \tag{18}$$

Substituting (18) into the second of equations (15) we obtain

$$C_2'(y) + C_2(y)C_1'(y)x = \alpha[U'(y)]^{p-1}C_2(y)C_1(y) \tag{19}$$

The right-hand side of (19) is independent of x. Therefore $C_1'(y) = 0$ and

$$C_1(y) = \frac{1}{2}\frac{d}{dy}\ln\left|\frac{1+\alpha[U']^{p-1}}{1-\alpha[U']^{p-1}}\right| = \frac{C_0}{2} = \text{const.} \tag{20}$$

so that

$$\Pi(x,y) = C_2(y)e^{C_0 x/2}\,, \quad C_2(0) = 1\,. \tag{21}$$

Integrating (20) in y and taking into account that $\alpha U' > 0$ obtain

$$\frac{1+\alpha[U']^{p-1}}{1-\alpha[U']^{p-1}} = M_{1,2}e^{C_0 y}\,, \tag{22}$$

where $M_1 < 0$ and $M_2 > 0$ are chosen for $\alpha[U']^{p-1} > 1$ and $\alpha[U']^{p-1} < 1$, respectively. Given that the right-hand side of equation (22) is non-singular for any finite $M_{1,2}$ and C_0 we conclude that the velocity profile must be such that the condition $\alpha[U']^{p-1} > 1$ or $\alpha[U']^{p-1} < 1$ is satisfied everywhere in the flow. Also note that the absolute value of the ratio in the left-hand side of equation (22) is greater than 1 for all positive values of α and U'. On the other hand the term $e^{C_0 y}$ in the right-hand side ranges from values which are less than 1 to values which are greater than 1 over the interval $-1 \le y \le 1$ for any value of C_0. Therefore the balance between the left- and right-hand sides of equation (22) can only be achieved if

$$|M_{1,2}| > e^{|C_0|} \ge 1\,. \tag{23}$$

This condition apparently was overlooked in the original work by Hron et al. [1] which ultimately resulted in their incorrect conclusion regarding the possibility of inflection-point solutions for the problem. This will be discussed in more detail in Section 3.1.

Rearranging equation (22) we obtain

$$U'(y) = \left(\frac{1}{\alpha}\frac{M_{1,2}e^{C_0 y} - 1}{M_{1,2}e^{C_0 y} + 1}\right)^{\frac{1}{p-1}}\,. \tag{24}$$

Since $U(-1) = 0$ the expression for the basic flow velocity is given by

$$U(y) = \int_{-1}^{y} \left(\frac{1}{\alpha}\frac{M_{1,2}e^{C_0 s} - 1}{M_{1,2}e^{C_0 s} + 1}\right)^{\frac{1}{p-1}} ds\,. \tag{25}$$

The substitution of (24) and (20) into (19) results in

$$\frac{C_2'(y)}{C_2(y)} = \frac{C_0}{2}\left[\frac{M_{1,2}e^{C_0 y} - 1}{M_{1,2}e^{C_0 y} + 1}\right]\,. \tag{26}$$

Integrating (26) with respect to y and taking into account that $C_2(0) = 1$ we obtain

$$C_2(y) = \frac{M_{1,2}e^{C_0 y/2} + e^{-C_0 y/2}}{M_{1,2} + 1}\,,$$

so that the final expression for the pressure is

$$\Pi(x,y) = \frac{M_{1,2} + e^{-C_0 y}}{M_{1,2} + 1} e^{C_0(x+y)/2}\,. \tag{27}$$

It follows from this expression that the sign of constant C_0 defines the direction of the applied pressure gradient and thus the preferable direction for the pressure-driven flow (left–right if $C_0 < 0$ and right–left if $C_0 > 0$). Also note

that restrictions (23) guarantee that the pressure (and thus the fluid viscosity) remain positive in the flow domain.

In conclusion of this section we provide useful asymptotic expressions for the velocity and pressure fields obtained from equations (25) and (27) in the limit of $C_0 \to 0$:

$$\begin{aligned} U(y) \approx & \left(\frac{1}{\alpha}\frac{M_{1,2}-1}{M_{1,2}+1}\right)^{\frac{1}{p-1}}(y+1) \\ & + \left(\frac{(M_{1,2}-1)^{2-p}}{\alpha(M_{1,2}+1)^p}\right)^{\frac{1}{p-1}} \frac{M_{1,2}C_0}{p-1}(y^2-1) \\ & + \left(\frac{(M_{1,2}-1)^{3-2p}}{\alpha(M_{1,2}+1)^{2p-1}}\right)^{\frac{1}{p-1}} \frac{M_{1,2}C_0^2}{3(p-1)^2}[(M_{1,2}+1)^2 - p(M_{1,2}^2+1)](y^3+1)\,, \end{aligned} \tag{28}$$

where $M_{1,2}$ are determined from the boundary condition $U(1) = V$ and

$$\Pi(x,y) \approx 1 + \left(x + y - \frac{2y}{M_{1,2}+1}\right)\frac{C_0}{2} + \left[\frac{(x+y)^2}{4} - \frac{xy}{M_{1,2}+1}\right]\frac{C_0^2}{2}\,. \tag{29}$$

Note that in general the pressure depends on the value of p implicitly via the values of $M_{1,2}$. For definiteness and unless specified otherwise in the text we will take $C_0 < 0$ in the subsequent discussion. This corresponds to a negative longitudinal pressure gradient assisting a left-to-right flow.

3.1 Inflection point profiles are impossible for a shear-thinning fluid

Some of the velocity profiles for Couette-Poiseuille flow presented by Hron et al. [1] in their Figure 4 contain an inflection point within the flow domain. While providing the values of C_0, p and V for their fields these authors do not give the corresponding values of α and thus it is impossible to reproduce their solutions exactly. Therefore we only sketch them in Figure 1 for reference convenience. Below we will argue that the inflection velocity profiles such as the ones reported in [1] and sketched in Figure 1(*a*,*b*) cannot satisfy the governing equations (15) for shear-thinning fluid with $1 < p < 2$ and therefore are incorrect.

Differentiating equation (24) with respect to y leads to

$$U''(y) = \frac{2C_0M_2e^{C_0y}}{(p-1)\alpha^{1/(p-1)}}\frac{\left(M_2e^{C_0y}-1\right)^{(2-p)/(p-1)}}{(M_2e^{C_0y}+1)^{p/(p-1)}}\,. \tag{30}$$

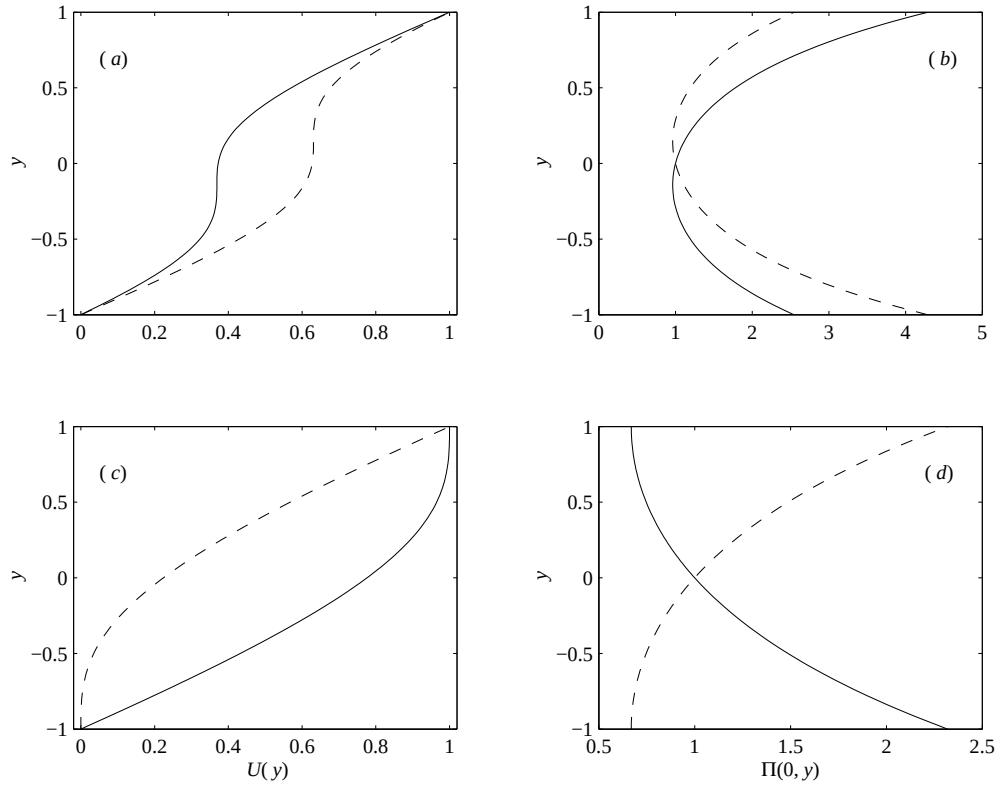

Fig. 1. Sketch of some Couette-Poiseuille solutions reported in [1] for $C_0 < 0$ and $p = \frac{3}{2}$: (a), (c) the velocity and (b), (d) the corresponding pressure profiles.

We only consider the solution with $M_2 > 0$ because the necessary inflection point condition $U''(Y) = 0$ cannot be satisfied for $M_1 < 0$ at any y. Note from equations (24) and (30) that if Y is an inflection point so that $U''(Y) = 0$ then $U'(Y) = 0$ as well. The profiles depicted in Figure 4 in [1] (see the sketch in Figure $1(a)$) seem to confirm this. However condition (23) means that $M_2 e^{C_0 y} - 1 \geq 0$ for $-1 \leq y \leq 1$ and according to equation (30) $U''(y)$ cannot change its sign within the flow domain. Therefore inflection profiles satisfying the Couette flow condition $U'(y) \geq 0$, $-1 \leq y \leq 1$ and similar in shape to those sketched in Figure $1(a)$ cannot exist. In this regard Couette-type flows of a fluid with pressure dependent viscosity are similar to the corresponding flows of a Newtonian fluid.

The corollary of the above discussion is that the curvature of a monotonic velocity profile can be zero only at the boundaries $y = \pm 1$, see Figure 1(c).

3.2 Specific case of $p = 2$

For $p = 2$ the governing equations (1) take the form which is closest to Navier-Stokes equations describing flows of Newtonian fluids. Shear-thickening or

shear-thinning is not present in this case and therefore we consider it in detail first in order to highlight the major effects brought about by the dependence of the viscosity on the pressure. Equation (25) results in

$$U(y) = -\frac{1+y}{\alpha} + \frac{2}{\alpha C_0} \ln \frac{M_{1,2} e^{C_0 y} + 1}{M_{1,2} e^{-C_0} + 1}\,, \quad M_{1,2} = \frac{1 - e^{\frac{\alpha V + 2}{2} C_0}}{e^{\frac{\alpha V}{2} C_0} - e^{C_0}}\,, \tag{31}$$

where $M_{1,2} \lessgtr 0$ is chosen for $\alpha V \gtrless 2$, respectively. It is easy to show that the condition $|M_1| > e^{|C_0|}$ is satisfied for any value of $C_0 < 0$. In other words we arrive at a remarkable and somewhat counterintuitive conclusion that if the upper wall velocity is greater than the critical speed $V_c = 2/\alpha$ the Couette condition $U'(y) \geq 0$ is satisfied everywhere in the flow domain regardless of how strong the applied longitudinal pressure gradient is. This behaviour is caused completely by the piezo-viscosity and is drastically different from that of fluids with pressure-independent viscosity. As seen from Figure 2(a,b) strengthening the longitudinal pressure gradient leads to the formation of a thin velocity boundary layer near the moving plate where the viscosity is significantly smaller than that in the bulk of the fluid. The upper plate essentially slides along the surface of the fluid whose bulk moves with an invariant linear velocity profile given by (14). Increasing the pressure effectively "freezes" the fluid making it more viscous in the bulk so that a high-velocity motion only exists near the moving boundary. The linear part of the velocity profiles shown in Figure 2(a) remains invariant when $|C_0|$ is sufficiently large while the pressure distribution shown in Figure 4(b) changes very strongly. Such a behaviour becomes possible only because of the pressure's non-uniqueness in the critical regime discussed in the beginning of Section 3. In other words, various solutions for Π given by (14) can be considered as the pressure distributions corresponding to velocity profiles which are distinct in principle, but the difference between which is exponentially small.

For small wall velocities $V < 2/\alpha$ the condition $M_2 > e^{|C_0|}$ is only satisfied for $|C_0| < K$, where K is given by equation

$$\cosh K = e^{\frac{\alpha V K}{2}}\,, \text{ or, when } \alpha V \to 0\,, \quad K \approx \alpha V\,. \tag{32}$$

A family of low-speed Couette-type flows is shown in Figure 2(c,d). As for fluids with pressure-independent viscosity, increasing the pressure gradient leads to a larger curvature of the velocity profile near the moving wall.

For $|C_0| > K$ the Couette condition $U'(y) \geq 0$ cannot be satisfied for all coordinates y. Therefore in these regimes strengthening the pressure gradient will lead to the appearance of the velocity profiles containing segments of positive and negative shear as is the case in Poiseuille-type flows. These flows will be considered in detail in Section 4.1. The parametric boundary between Couette- and Poiseuille-type flows is shown in Figure 3(a). It has a vertical asymptote at $\alpha V = 2$ to the right of which only a Couette-type flow with $U'(y) > 0$ is

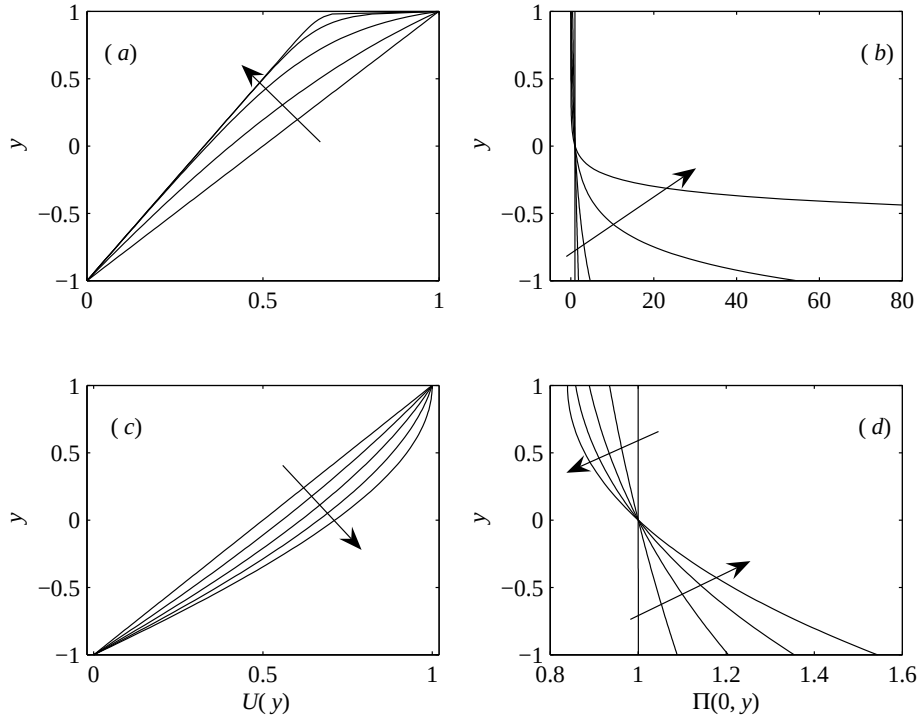

Fig. 2. Couette-type solutions for $p = 2$ and $V = 1$: (a), (b) $\alpha = 3$, $C_0 = 0, -1, -3, -8, -20$; (c), (d) $\alpha = 1$, $C_0 = -iK/4$, $i = 0, 1, 2, 3, 4$, $K \approx 1.2188$. Arrows indicate the direction of increasing $|C_0|$.

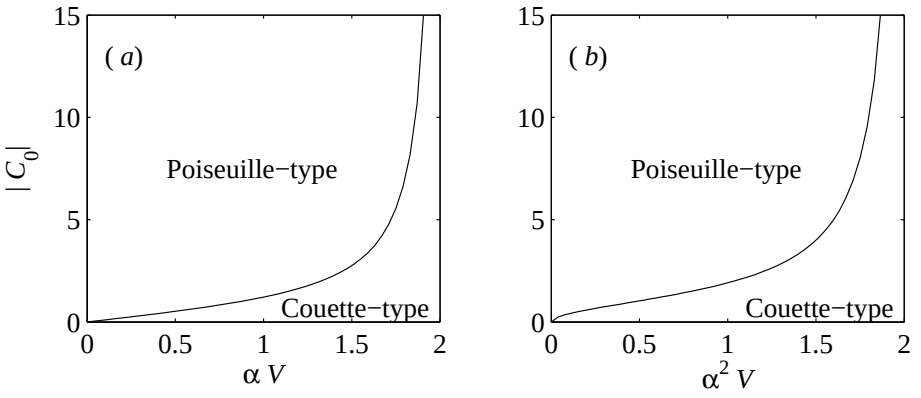

Fig. 3. The boundary $|C_0| = K$ given by equations (32) and (42) separating Couette- and Poiseuille-type solutions for (a) $p = 2$ and (b) $p = \frac{3}{2}$.

possible, the feature not found for fluids with pressure-independent viscosity.

In the limit of $C_0 \to 0$ which corresponds to small pressure gradients along the channel the series expansions (28) and (29) with $p = 2$ and expression (31) for $M_{1,2}$ become

$$M_{1,2} \approx \frac{2+\alpha V}{2-\alpha V}\left(1+\frac{\alpha V C_0^2}{12}\right), \tag{33}$$

$$U(y) \approx V\frac{y+1}{2} + \frac{C_0}{16\alpha}(4-\alpha^2V^2)(y^2-1)\left(1+\frac{C_0 V y}{6}\right), \tag{34}$$

$$\Pi(x,y) \approx 1 + \frac{C_0}{4}(2x+\alpha V y) + \frac{C_0^2}{8}(x^2+y^2+\alpha V x y). \tag{35}$$

As expected, by setting $C_0 = 0$ we recover plane Couette flow of Newtonian fluid

$$\Pi = 1, \quad U(y) = V\frac{y+1}{2}. \tag{36}$$

The terms linear in C_0 lead to the expressions similar to those for Couette-Poiseuille flows of fluids with pressure-independent viscosity while terms quadratic in C_0 introduce piezo-viscous effects.

3.3 Specific case of $p = \frac{3}{2}$

In the case of $p = \frac{3}{2}$ considered in [1] equation (25) leads to the following expression for the basic velocity profile

$$U(y) = \frac{y+1}{\alpha^2} - \frac{4M_{1,2}}{\alpha^2 C_0}\frac{e^{C_0 y} - e^{-C_0}}{(M_{1,2}e^{-C_0}+1)(M_{1,2}e^{C_0 y}+1)}. \tag{37}$$

The boundary condition $U(1) = V$ then leads to

$$V = \frac{2}{\alpha^2} - \frac{8M_{1,2}}{\alpha^2 C_0}\frac{\sinh C_0}{(M_{1,2}e^{-C_0}+1)(M_{1,2}e^{C_0}+1)} \tag{38}$$

and a quadratic equation for $M_{1,2}$

$$M_{1,2}^2 + 2\delta M_{1,2} + 1 = 0, \quad \delta = \cosh C_0 + \frac{4}{\alpha^2 V - 2}\frac{\sinh C_0}{C_0}. \tag{39}$$

The real solutions exist only if $|\delta| \geq 1$ and only those of them which lead to $|M_{1,2}| > e^{|C_0|}$ are relevant. Therefore

$$\alpha^2 V > 2: \quad \delta > 1, \quad M_1 = -\delta - \sqrt{\delta^2-1} < -e^{|C_0|}, \tag{40}$$

$$\alpha^2 V < 2: \ \delta < -1, \ M_2 = -\delta + \sqrt{\delta^2-1} > e^{|C_0|}. \tag{41}$$

Subsequently, we conclude that for any fixed set of parameters (α, V, C_0) there exists a unique basic flow velocity profile satisfying the condition $U' > 0$ for $-1 \leq y \leq 1$. This is in contrast to the conclusion made in [1] that multiple solutions to the problem are possible. For example, it is claimed in [1] that two distinct solutions with monotonic velocity profiles sketched in Figure 1(c) and

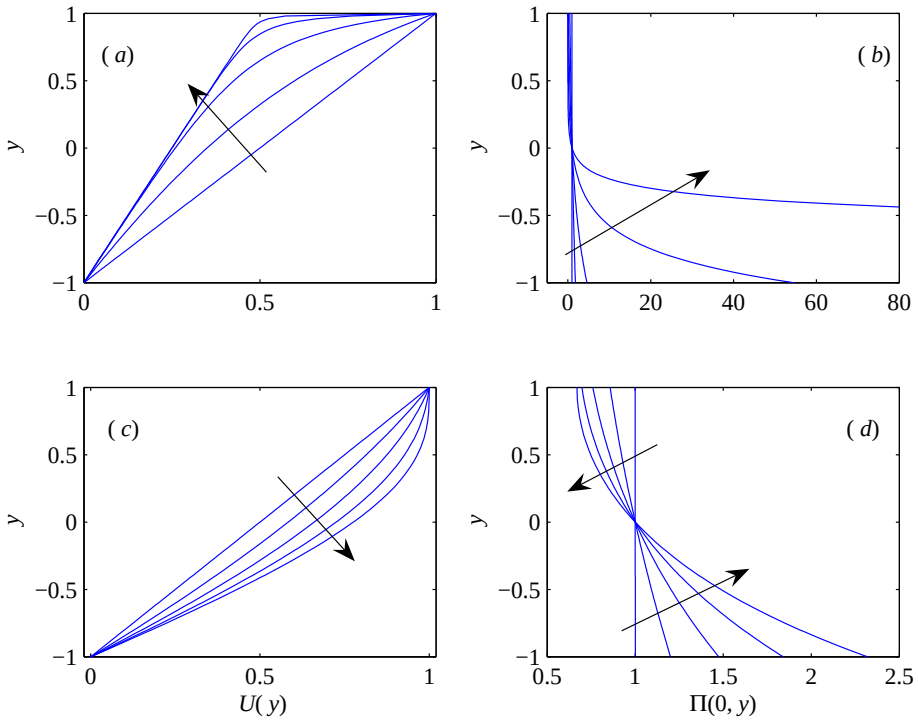

Fig. 4. Couette-type solutions for $p = \frac{3}{2}$ and $V = 1$: (a), (b) $\alpha = 2$, $C_0 = 0, -1, -3, -8, -20$; (c), (d) $\alpha = 1$, $C_0 = -iK/4$, $i = 0, 1, 2, 3, 4$, $K \approx 1.9150$. Arrows indicate the direction of increasing $|C_0|$.

the corresponding pressure distributions shown in Figure 1(d) can exist for the same set of physical parameters for $p = \frac{3}{2}$ and $C_0 < 0$. However it is easy to see that solutions similar to those shown by the dashed lines in Figure 1(c,d) do not satisfy the governing equations (15). Indeed for $C_0 < 0$ the longitudinal pressure gradient $\frac{\partial \Pi}{\partial x}$ is negative. At the same time for the solution showed by the dashed-line $\frac{\partial \Pi}{\partial y} > 0$ and $U' > 0$. Therefore the second of equations (15) cannot be satisfied since its left- and right-hand sides have opposite signs. Thus like in the case of Newtonian fluids, only one solution (sketched by a solid line in Figure 1(c,d)) can exist. See also a similar discussion in [17].

Now consider the limitations imposed by inequalities (40) in more detail. It follows from definition (39) that $\delta > \cosh C_0 \geq 1$ for any C_0. Re-write the second of inequalities (40) as

$$\sqrt{\delta^2 - 1} > e^{|C_0|} - \delta = \left(1 - \frac{4}{(\alpha^2 V - 2)|C_0|}\right) \sinh |C_0| \,.$$

It is clearly satisfied if the expression in parentheses is negative. If it is positive

the above is equivalent to

$$\frac{8\sinh|C_0|\cosh|C_0|}{(\alpha^2V-2)|C_0|} > -\frac{8\sinh^2|C_0|}{(\alpha^2V-2)|C_0|}$$

which is also satisfied for any C_0. Similarly to the case of $p = 2$ we conclude that if the upper plate moves with a speed which is larger than $V_c = 2/\alpha^2$ the velocity profile remains monotonic with $U' > 0$ regardless of how strong the applied pressure gradient is. As seen from Figure 4(a,b) strengthening of the longitudinal pressure gradient also leads to the formation of a thin velocity boundary layer near the moving plate and all velocity and pressure distributions obtained for $p = 3/2$ are remarkably similar to those found for $p = 2$. Therefore the shear-thinning properties of the fluid have little influence on the flow behaviour in comparison with piezo-viscous effects.

If the velocity of the upper plate is smaller than the critical value then the influence of the applied pressure gradient is more conventional: it leads to the curvature variation of the bulk velocity profile as seen in Figure 4 (c,d). A monotonic velocity profile can only exist until $U'(1)$ becomes zero which corresponds to the smallest allowed value of $M_2 = e^{|C_0|}$. Upon using (39) and (40) we find that the maximum value of $|C_0| = K$ for which the Couette condition $U' \geq 0$ is still fulfilled has to satisfy the equation

$$K = \frac{2\tanh K}{2-\alpha^2V} \quad \text{or, when } \alpha^2V \to 0\,, \quad K \approx \alpha\sqrt{\frac{3V}{2}}\,. \tag{42}$$

If $V < V_c$ and $|C_0| > K$ then the velocity profile cannot be monotonic anymore. The applied pressure gradient becomes too strong and the basic flow velocity profile will have regions of positive and negative slopes similar to those in a plane Poiseuille flow of Newtonian fluids. Such profiles cannot be described by equation (25) having a constant $M_{1,2}$ uniquely defined for the complete flow region and require a slightly different treatment as will be described in Section 4. The diagram showing the parametric boundary separating Couette- and Poiseuille-type flows for $p = 3/2$ is shown in Figure 3(b). It is very similar to the diagram depicted in Figure 3(a) for $p = 2$. The same can be said about the velocity profiles. Therefore we conclude that the major qualitative flow features are defined by the piezo-viscosity rather than by the shear-thinning ability of the fluid. The only difference seen from comparing Figures 2 and 4 (c) is that shear-thinning leads to a slightly fuller velocity profile near the moving wall because a small-shear region tends to move as a solid due to the increased viscosity.

In the limit of $C_0 \to 0$ the series expansions (28) and (29) with $p = 3/2$ and expressions (40) and (41) become

$$M_{1,2} \approx \frac{\sqrt{2}+\alpha\sqrt{V}}{\sqrt{2}-\alpha\sqrt{V}}\left(1+\frac{3\alpha^2V-2}{12\alpha\sqrt{2V}}C_0^2\right), \tag{43}$$

$$U(y) \approx V\frac{y+1}{2}+\frac{C_0\sqrt{2V}}{8\alpha}(2-\alpha^2V)(y^2-1) + \frac{C_0^2}{48\alpha^2}(2-\alpha^2V)(3\alpha^2V-2)y(y^2-1), \tag{44}$$

$$\Pi(x,y) \approx 1+\frac{C_0}{4}(2x+\sqrt{2V}\alpha y)+\frac{C_0^2}{8}(x^2+y^2+\sqrt{2V}\alpha xy). \tag{45}$$

Again, by setting $C_0 = 0$ we recover plane Couette flow (36), however the Couette-Poiseuille flow given by terms linear in C_0 is somewhat different from that arising at $p = 2$. This difference results from the shear-thinning effects observed at $p = 3/2$.

4 Poiseuille-type flows

For Poiseuille-type flows occuring when the applied pressure gradient is sufficiently strong and the wall velocity is smaller than the critical speed the velocity profile will have an extremum at some interior point Y, $-1 < Y < 1$, where $U'(Y) = 0$. If $\frac{\partial\Pi}{\partial x} < 0$ we expect that $U'(y) \lesseqgtr 0$ for $y \gtreqless Y$. For $\frac{\partial\Pi}{\partial x} > 0$ the signs of the velocity derivatives will be reversed. Consider the case of $\frac{\partial\Pi}{\partial x} < 0$ (i.e. $C_0 < 0$) first.

For $-1 \le y < Y$, $U' > 0$ so that equations (13)–(22) hold. Equation (22) immediately gives $M_{1,2} = e^{-C_0Y}$ and then for $-1 \le y \le Y$ the solution is

$$U(y) = \int_{-1}^{y}\left(\frac{1}{\alpha}\frac{e^{C_0(s-Y)}-1}{e^{C_0(s-Y)}+1}\right)^{\frac{1}{p-1}} ds, \quad \Pi(x,y) = \frac{1+e^{C_0(Y-y)}}{1+e^{C_0Y}}e^{C_0(x+y)/2}. \tag{46}$$

For $Y < y \le 1$, $U' = -|U'| < 0$ so that equations (13) become

$$\frac{\partial\Pi}{\partial x}+\alpha\frac{\partial}{\partial y}\left(\Pi|U'|^{p-1}\right) = 0, \quad \frac{\partial\Pi}{\partial y}+\alpha\frac{\partial}{\partial x}\left(\Pi|U'|^{p-1}\right) = 0. \tag{47}$$

A solution procedure similar to that described in Section 3 results in the following expressions for the velocity and the pressure valid in the region $Y \le y \le 1$

$$U(y) = V+\int_{y}^{1}\left(\frac{1}{\alpha}\frac{1-e^{C_0(s-Y)}}{1+e^{C_0(s-Y)}}\right)^{\frac{1}{p-1}} ds, \quad \Pi(x,y) = \frac{1+e^{C_0(Y-y)}}{1+e^{C_0Y}}e^{C_0(x+y)/2}. \tag{48}$$

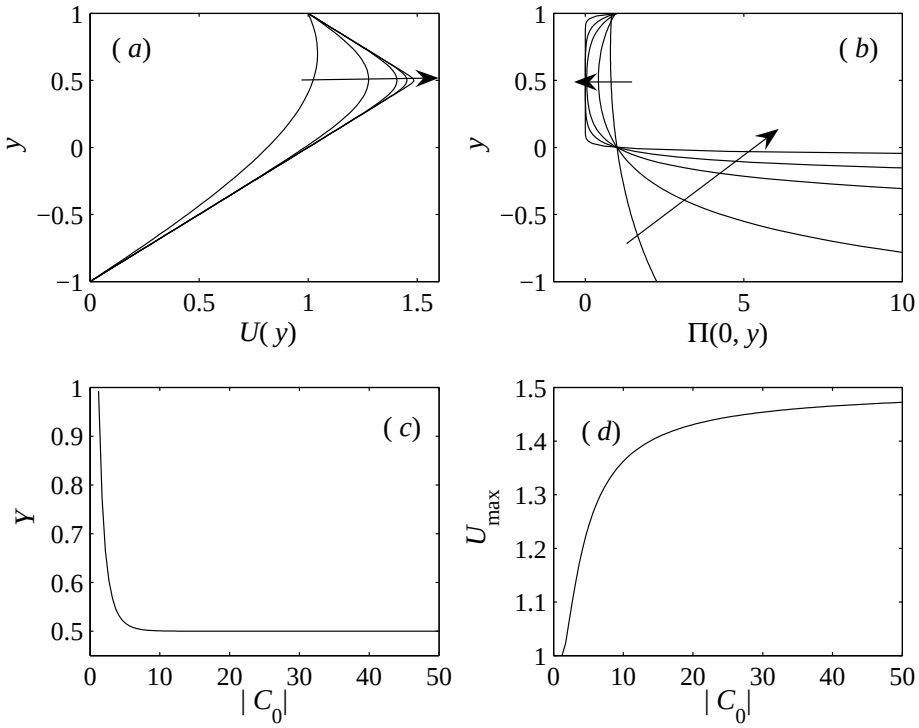

Fig. 5. Poiseuille-type solutions for $p = 2$ and $\alpha = V = 1$: (a) velocity, (b) pressure for $C_0 = -2, -6, -15, -30, -100$; ($c$), location of the velocity maximum and (d) the maximum velocity as the function of $|C_0|$. Arrows indicate the direction of increasing $|C_0|$.

Note that the values of C_0 must be the same in equations (46) and (48) in order to guarantee the continuity of pressure. After integration in y the boundary conditions $U(-1) = 0$ and $U(1) = V$ and the continuity condition $U(Y_{+0}) = U(Y_{-0})$ fully define the velocity profile and the extremum location Y. Finally note that when $C_0 > 0$ the solution for the pressure is still given by equations (46) and (48) while the integrands in the velocity solutions (46) and (48) need to be swapped.

4.1 Specific case of $p = 2$

When $p = 2$, the integration of (46) and (48) leads to the expressions for the velocity profile which both can be written as

$$U(y) = \frac{1 - y + 2Y}{\alpha} + \frac{2}{\alpha C_0} \ln \frac{e^{C_0(y-Y)} + 1}{e^{C_0(1+Y)} + 1}, \quad Y = \frac{1}{C_0} \ln \frac{e^{C_0} - e^{\frac{\alpha V C_0}{2}}}{e^{C_0 + \frac{\alpha V C_0}{2}} - 1} \quad (49)$$

which is valid for $-1 \leq y \leq 1$. A set of representative profiles is shown in Figure 5(a). For small pressure gradients the velocity profiles are quite similar

to those of Poiseuille-type flows of fluids with pressure-independent viscosity. However at larger values of $|C_0|$ the flow profiles of a piezo-viscous fluid are drastically different. They essentially consist of two linear segments corresponding to the critical velocity profile (14) with very large curvature in the region near $y = Y$ connecting them. The value of Y asymptotically approaches $Y = \frac{\alpha V}{2}$, see Figure 5(c), which is obtained as the limit of (49) as $C_0 \to -\infty$ when $\alpha V < 2$. Perhaps the most drastic distinction of the considered flow from its counterpart with the pressure-independent viscosity is the "choking" of the channel: regardless of how large the applied pressure gradient is the maximum flow velocity cannot exceed the asymptotic value of $U_{\max} = \frac{V}{2} + \frac{1}{\alpha}$, see Figure 5($d$). The pressure distribution shown in Figure 5(b) indicates that the fluid becomes less viscous near the moving wall while the viscosity near the stagnant wall, being a linear function of the pressure, increases drastically.

For pure Poiseuille flow ($V = 0$) we obtain $Y = 0$ and the velocity profile expression reduces to

$$U(y) = -\frac{y+1}{\alpha} + \frac{2}{\alpha C_0} \ln \frac{1 + e^{C_0 y}}{1 + e^{-C_0}} \equiv \frac{2}{\alpha C_0} \ln \frac{\cosh \frac{C_0 y}{2}}{\cosh \frac{C_0}{2}}\,, \tag{50}$$

which was originally derived in [1]. In the limit $C_0 \to 0$ we recover a parabolic profile corresponding to the flow of a Newtonian fluid with non-Newtonian contribution proportional to C_0^3

$$U(y) \approx \frac{y^2 - 1}{4\alpha} C_0 - \frac{y^4 - 1}{96\alpha} C_0^3\,. \tag{51}$$

The maximum flow speed achieved at $y = 0$ in this limit is

$$U_{\max} \approx -\frac{C_0}{4\alpha}\left(1 - \frac{C_0^2}{24}\right)$$

which shows that non-Newtonian effects are characterised by the magnitude of the term $C_0^2/24$. For a more straightforward comparison of our solutions with conventionally non-dimensionalised flows of Newtonian fluids note that a standard definition of Reynolds number Re^* is obtained using (12) as follows

$$Re^* = \frac{\rho U_{\max} u^* L}{\mu^*} = -\frac{\rho C_0 u^* L}{4\alpha\mu^*} = -\frac{C_0}{4\alpha^2} = -\frac{C_0}{4} Re^2\,.$$

4.2 Specific case of $p = 3/2$

With $p = \frac{3}{2}$ the integration of equations (46) and (48) leads to the following basic velocity profile for Poiseuille-type flows

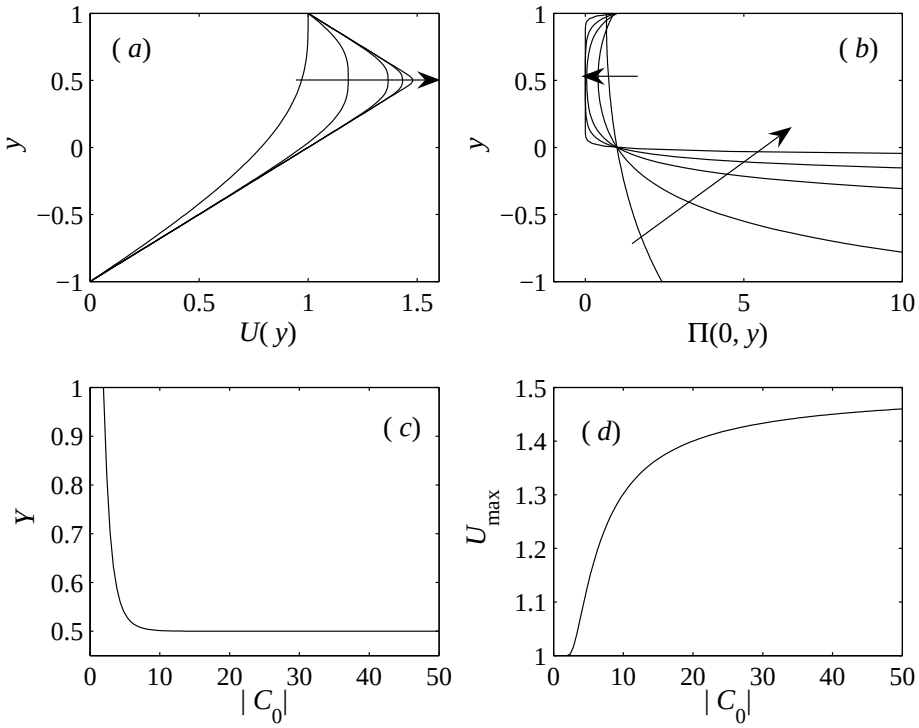

Fig. 6. Poiseuille-type solutions for $p = \frac{3}{2}$ and $\alpha = V = 1$: (a) velocity, (b) pressure for $C_0 = -2, -6, -15, -30, -100$; ($c$), location of the velocity maximum and (d) the maximum velocity as the function of $|C_0|$. Arrows indicate the direction of increasing $|C_0|$.

$$U(y) = -\frac{1+y}{\alpha^2}\frac{C_0}{|C_0|} - \frac{4}{\alpha^2|C_0|}\frac{1-e^{C_0(y+1)}}{\left(1+e^{C_0(y-Y)}\right)\left(1+e^{C_0(Y+1)}\right)}\,,\ -1 \le y \le Y\,,$$

$$U(y) = V - \frac{1-y}{\alpha^2}\frac{C_0}{|C_0|} + \frac{4}{\alpha^2|C_0|}\frac{1-e^{C_0(y-1)}}{\left(1+e^{C_0(y-Y)}\right)\left(1+e^{C_0(Y-1)}\right)}\,,\ Y \le y \le 1\,,$$

where the extremum coordinate Y satisfies the equation

$$\frac{4\sinh(C_0 Y)}{\cosh(C_0 Y) + \cosh C_0} - 2C_0 Y = \alpha^2 V|C_0|\,. \tag{52}$$

A family of representative solutions is shown in Figure 6. Similarly to Couette-type flows, the velocity profiles differ drastically from their Newtonian counterparts. As for $p = 2$ the channel chokes for large values of $|C_0|$: no increase of the driving pressure gradient can lead to the maximum flow velocity greater than $U_{\max} = \frac{V}{2} + \frac{1}{\alpha^2}$ achieved at $Y_{\max} = \frac{\alpha^2 V}{2}$ in the limit $|C_0| \to \infty$, see Figure 6(c, d). The pressure distribution shown in Figure 6(b) is very similar to that found for $p = 2$.

In the limit of pure Poiseuille flow ($V = 0$) equation (52) results in $Y = 0$ and, after some trigonometric manipulations, the velocity profile can be re-written

as

$$U(y) = \frac{|y|-1}{\alpha^2}\frac{C_0}{|C_0|} + \frac{\tanh(C_0/2) - \tanh(C_0|y|/2)}{\alpha^2|C_0/2|}\,,\ -1 \le y \le 1\,. \qquad (53)$$

This is a generalisation of equation (3.20) given in [1]. For small values of $|C_0|$ expression (53) reduces to a power-law fluid profile

$$U(y) = \frac{|y|^3-1}{12\alpha^2}\,\frac{C_0^3}{|C_0|} \qquad (54)$$

with the maximum speed

$$|U_{\max}| \approx \frac{C_0^2}{12\alpha^2}\,.$$

Comparing this with the expression for $p = 2$ we conclude that due to the shear-thinning effects the maximum speed of pure Poiseille flow is larger for $p = \frac{3}{2}$ if the ratio $\frac{|C_0|}{\alpha} > 3$ i.e. for large longitudinal pressure gradients. For further discussion of the family of pure Poiseuille profiles the reader is referred to [1].

5 Conclusions

We have undertaken a thorough parametric study of unidirectional plane shear flows of an incompressible fluid with the pressure-dependent viscosity. It is shown that the problem is governed by three non-dimensional parameters: the wall speed V, C_0 characterising the applied pressure gradient and α representing the rheology of a fluid. We have found that in contrast to the previous reports [1,8] the flow solution is always unique for any fixed set of governing parameters and that solutions with velocity profiles containing an inflection point cannot exist. The obtained solutions reveal a drastic difference in the flow behaviour of a piezo-viscous fluid in comparison with its pressure-independent counterpart. The major features are: the existence of three classes of solutions (one Poiseuille- and two Couette-type flow families); the existence of the critical wall speed beyond which a new Couette-type solution (not found for fluids with pressure-independent viscosity) exists; and the channel choking phenomenon discovered in Poiseuille-type flows at large longitudinal pressure gradients. At the same time the comparison of solutions obtained for shear-independent ($p = 2$) and shear-thinning ($p = \frac{3}{2}$) piezo-viscous fluids reveals no qualitative difference between their flows. Given the drastic distinction between simple flows of pressure-independent and piezo-viscous fluids a hydrodynamic stability study of the considered flows reveals even more new features and provides further insight into their physics. This study is currently underway. The first results for pure Poiseuille flow are reported in [18]

and the results for Poiseuille-Couette flow will be presented in a subsequent publication.

References

[1] J. Hron, J. Málek, K. R. Rajagopal, Simple flows of fluids with pressure-dependent viscosities, Proc. R. Soc. Lond. A 457 (2001) 1603–1622.

[2] G. G. Stokes, On the theories of the internal friction of fluids in motion, and of the equilibrium and motion of elastic solids, Trans. Camb. Phil. Soc. 8 (1845) 287–305.

[3] T. W. Bridgman, The physics of high pressure, The MacMillan Company, New York, 1931.

[4] E. M. Griest, W. Webb, R. W. Schiessler, Effect of pressure on viscosity of higher hydrocarbons and their mixtures, J. Chem. Phys. 29 (1958) 711–720.

[5] F. Koran, J. M. Dealy, A high pressure sliding plate rheometry for polymer melts, J. Rheol. 43 (1999) 1279–1290.

[6] T. W. Bates, J. A. Williamson, J. A. Spearot, C. K. Murphy, A correlation between engine oil rheology and oil film thickness in engine journal bearing, Society of Automotive Engineers (1986) 860376.

[7] D. R. Gwynllyw, A. R. Davies, T. N. Phillips, On the effects of a piezoviscous lubricant on the dynamics of a journal bearing, J. Rheol. 40 (1996) 1239–1266.

[8] J. Málek, J. Necas, K. R. Rajagopal, Global analysis of the flows of fluids with pressure-dependent viscosities, Arch. Rational Mech. Anal. 165 (2002) 243–269.

[9] J. Málek, J. Necas, K. R. Rajagopal, Global existence of solutions for flows of fluids with pressure and shear dependent viscosities, Appl. Math. Lett. 15 (2002) 961–967.

[10] J. Hron, J. Málek, J. Necas, K. R. Rajagopal, Numerical simulations and global existence of solutions of two-dimensional flows of fluids with pressure and shear dependent viscosities, Math. Comput. Simulations 61 (2003) 297–315.

[11] M. Franta, J. Málek, K. R. Rajagopal, On steady flows of fluids with pressure- and shear-dependent viscosities, Proc. R. Soc. A 461 (2005) 651–670.

[12] K. R. Rajagopal, G. Saccomandi, Unsteady exact solution for flows of fluids with pressure-dependent viscosities, Math. Proc. R. Irish Academy 106A (2006) 115–130.

[13] M. Renardy, Some remark on the Navier-Stokes equations with a pressure-dependent viscosity, Comm. Partial Differential Equations 11 (1986) 779–793.

[14] F. Gazzola, A note on the evolution of Navier-Stokes equations with a pressure-dependent viscosity, Z. Angew. Math. Phys. 48 (1997) 760–773.

[15] G. Hay, M. E. Mackay, K. M. Awati, Y. Park, Pressure and temperature effects in slit rheometry, J. Rheol. 43 (1999) 1099–1116.

[16] M. Renardy, Parallel shear flows of fluids with a pressure-dependent viscosity, J. Non-Newtonian Fluid Mech. 114 (2003) 229–236.

[17] R. R. Huilgol, Z. You, On the importance of the pressure dependence of viscosity in steady non-isothermal shearing flows of compressible and incompressible fluids and in the isothermal fountain flow, J. Non-Newtonian Fluid Mech. 136 (2006) 106–117.

[18] T. D. Tran, S. A. Suslov, Stability of plane Poiseuille flow of a fluid with pressure dependent viscosity, in: Proceedings of ICTAM08, International Congress on Theoretical and Applied Mechanics, Adelaide, Australia, ISBN 978-0-9805142-0-9, 2008.